LES MODELLING OF HYDROGEN RELEASE AND ACCUMULATION WITHIN A NON-VENTILATED AMBIENT PRESSURE GARAGE USING THE ADREA-HF CFD CODE

Koutsourakis, N.[1], Venetsanos, A.G.[2] and Bartzis, J.G.[3]
[1] Department of Mechanical Engineering, University of West Macedonia, Kozani, 50100, Greece, nk@ipta.demokritos.gr
[2] Environmental Research Laboratory, NCSR Demokritos, Aghia Paraskevi, 15310, Greece, venets@ipta.demokritos.gr
[3] Department of Mechanical Engineering, University of West Macedonia, Kozani, 50100, Greece, bartzis@uowm.gr

ABSTRACT

Computational Fluid Dynamics (CFD) has already proven to be a powerful tool to study the hydrogen dispersion and help in the hydrogen safety assessment. In this work, the Large Eddy Simulation (LES) recently incorporated into ADREA-HF CFD code is evaluated against the INERIS-6C experiment, which provides detailed experimental measurements, visualization of the flow and availability of previous CFD results from various institutions (HySafe SBEP-V3). The short-term evolution of the hydrogen concentrations in this confined space is examined and comparison with experimental data is provided, along with comments about the ability of LES to capture the transient phenomena occurring during hydrogen dispersion.

1.0 INTRODUCTION

CFD is a very powerful and relatively low-cost tool that can help in examining various hydrogen dispersion scenarios and support not only design procedures, but also decision making and emergency response. CFD can be thus considered a strategic means for the hydrogen safety assessment. The most common approach of this numerical method is the Reynolds Averaged Navier Stokes (RANS) technique, that has historically accompanied CFD from its very early stages. On the other hand, RANS is not very suitable for transient calculations, since it is based on averaging and it also models the whole turbulence spectra. A more recent approach is the LES, which is natively transient and solves explicitly the bigger, energy containing eddies. Low-cost computational power increase has made LES an attractive alternative CFD approach, despite the fact that LES needs substantially more calculation time than RANS.

Given the fact that the LES methodology has a high potential, it has been recently incorporated into ADREA-HF, which is a well-established CFD code in atmospheric and hydrogen release dispersion applications [1, 2]. The LES ability of ADREA-HF has already been evaluated against both flow field [3, 4] and pollutant dispersion [5] calculations. In this work, the new ADREA-HF LES code is used for the first time in hydrogen release calculations and the results are compared with experimental data.

2.0 DESCRIPTION OF THE EXPERIMENT

The experiment simulated was INERIS-TEST-6C, performed by INERIS within the activity InsHyde, internal project of the HySafe network of excellence. The purpose of the experiment was to evaluate the CFD codes in predicting the short and long term mixing and distribution of hydrogen releases in confined spaces.

The INERIS experiment was conducted in a rock cave of an approximately rectangular shape of dimensions 3.78 x 7.2 x 2.88 m in width, length and height respectively [6, 7] (Fig. 1). At a more or less central point of this supposed garage, at 3.8 m from the front side and 0.265 m from the floor, a 1 g/s vertical hydrogen release for 240 s from an orifice of 20 mm diameter was realized. The front side

of the room consisted of a sealed plastic wall, with two small openings at the bottom to assure constant (ambient) pressure. During the test, hydrogen concentration was measured regularly at 12 positions in the garage (Fig. 1), for a period up to 5160 s after the end of release, covering both the release and the subsequent diffusion phases. Fig. 2 presents photos from both the inside and outside of the room.

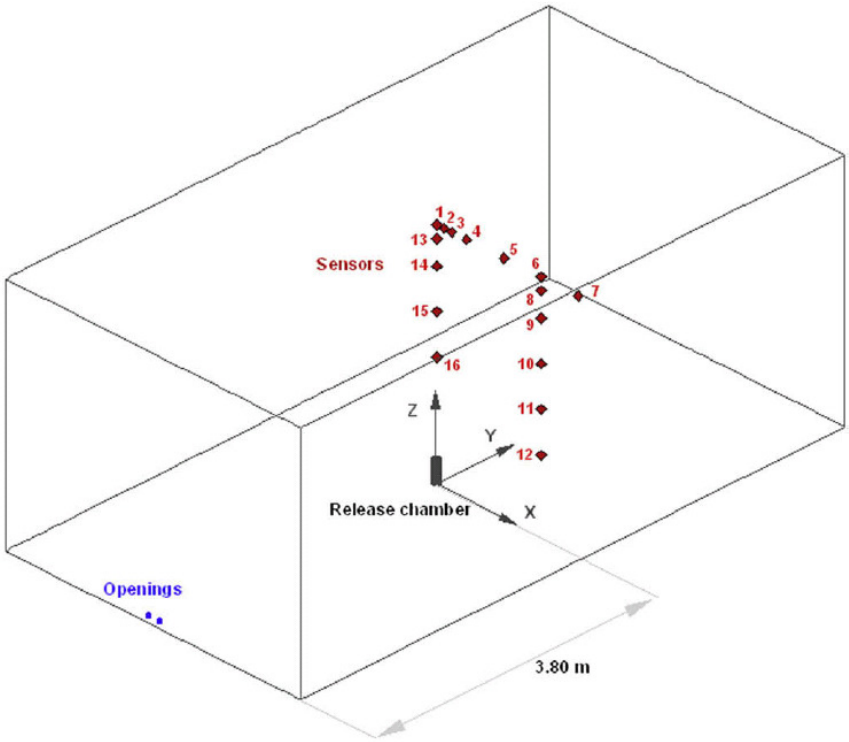

Figure 1. Geometry of the experiment garage and locations of the sensors (from [7])

Figure 2. Photos from inside and outside of the experimental cave

Before and after the experiment, the inter-comparison exercise SBEP-V3 was performed within the activity InsHyde [7], which helped in obtaining consensus regarding issues associated with prediction of hydrogen releases in confined spaces. CFD results were in general quite good, while the turbulence model, the resolution and the discretization scheme were the most important simulation parameters.

3.0 NUMERICAL METHODOLOGY

3.1 Governing equations

In LES, the large turbulent scales containing most of the energy are resolved explicitly, while only the Sub-Grid Scales (SGS) containing a small fraction of the energy are modeled. A spatial filtering is applied to every variable of the flow field, decomposing it into a resolved (of filtered) component and an SGS component. The filtered governing equations neglecting the terms not used in this study, are:

$$\frac{\partial \overline{\rho}}{\partial t} + \frac{\partial (\overline{\rho}\tilde{u}_i)}{\partial x_i} = 0\,, \tag{1}$$

$$\frac{\partial (\overline{\rho}\tilde{u}_i)}{\partial t} + \frac{\partial (\overline{\rho}\tilde{u}_i\tilde{u}_j)}{\partial x_j} = -\frac{\partial \overline{p}}{\partial x_i} + \frac{\partial (\tilde{\tau}_{ij}^{l} + \tau_{ij}^{R})}{\partial x_j}\,;\ \tilde{\tau}_{ij}^{l} + \frac{2}{3}\mu\frac{\partial \tilde{u}_k}{\partial x_k}\delta_{ij} = 2\mu\tilde{S}_{ij}\,;\ \tilde{S}_{ij} = \frac{1}{2}\left(\frac{\partial \tilde{u}_i}{\partial x_j} + \frac{\partial \tilde{u}_j}{\partial x_i}\right), \tag{2}$$

$$\overline{p} = \overline{\rho} r \overline{T}\,, \tag{3}$$

where ρ - density, kg/m^3; t - time, s; u_i - velocity components, m/s; x_i - distance, m; p - pressure, kg/ms^2; τ_{ij} - stress tensor components, kg/ms^2; μ - kinematic viscosity, kg/ms; δ_{ij} - Kronecker delta; S_{ij} - rate-of-strain tensor, s^{-1}; r - gas constant, m^2/K s^2; T - absolute temperature, K.

The instantaneous variables here are space-averaged and not time-averaged as in RANS, while the tilde denotes density weighted Favre-averaging. $\tilde{\tau}_{ij}^{l}$ is the instantaneous shear stress tensor due to molecular forcing and $\tau_{ij}^{R} = -\overline{\rho}\widetilde{u_i u_j} + \overline{\rho}\tilde{u}_i\tilde{u}_j$ is the residual stress tensor due to the subgrid turbulence, modeled using the classical Smagorinsky subgrid scale model, as:

$$\tau_{ij}^{R} + \frac{1}{3}\tau_{kk}\delta_{ij} = 2\mu_t\tilde{S}_{ij}\,;\ \mu_t = \overline{\rho}(C_s\Delta)^2\sqrt{2\tilde{S}_{ij}\tilde{S}_{ij}}\,, \tag{4}$$

The Smagorinsky constant C_s has a default value of 0.1. The term $\frac{1}{3}\tau_{kk}\delta_{ij}$, usually negligible compared to thermodynamic pressure [8], is incorporated into the filtered pressure. The filter-related Δ is taken as $\Delta = V^{1/3}$, where V is the volume of the computational cell. Near the solid boundaries, Van-Driest dumping was used [9], in order to account for the reduced growth of the small scales near the wall.

In ADREA-HF, the filtered scalar mass transport equation for a passive component i of a mixture, is:

$$\frac{\partial (\overline{\rho}\tilde{q}_i)}{\partial t} + \frac{\partial (\overline{\rho}\tilde{u}_j\tilde{q}_i)}{\partial x_j} = \frac{\partial}{\partial x_j}\left(\left(\overline{\rho}D_i + \frac{\mu_{sgs}}{Sc_{sgs}}\right)\frac{\partial \tilde{q}_i}{\partial x_j}\right), \tag{5}$$

where q_i - mass fraction of the component i; D_i - molecular diffusivity of the component i, m^2/s; μ_{sgs} - subgrid-scale kinematic viscosity, kg/ms; Sc_{sgs} - turbulent subgrid scale Schmidt number, 0.72. In this equation the modelling of the subgrid-scale scalar stress via an eddy gradient diffusion hypothesis is incorporated.

3.2 The numerical tools

ADREA-HF uses the finite volume method on a staggered Cartesian grid, while the geometry is plunged into the grid with the use of porosities, which makes possible the accurate representation of any solid surface on a structured mesh [1]. The pressure and velocity equations are decoupled with the use of the ADREA/SIMPLER algorithm [10]. For the discretization of the convective terms a second order accurate deferred correction central scheme [11] was used, providing a very good compromise between numerical stability and accuracy. For the time advancement, a second order accurate Crank-

Nicolson numerical scheme was chosen. For the concentration calculation, a second order accurate linear upwind scheme was used, along with a VanLeer limiter in order to increase the numerical stability. ADREA-HF is parallelized in both shared memory architectures with the use of OpenMP directives and in distributed memory architectures, using MPI. For the current runs, the Krylof subspace method BiCGstab was used, with the additive Schwarz preconditioner [12]. Both the creation of the preconditioner and the solution of the preconditioner system are done in parallel. The simulation reported here took about 15 days for the first 240 seconds of the experiment, in a modern quad-core personal computer. Then the time step increased and only about two more days were needed for the next 260 seconds.

3.3 The simulation approach

The whole experimental room was simulated, while the computational domain extended for 5.9 meters outside the front wall, in order to avoid possible effects due to the outflow from the pressure equilibrium openings. The number of cells in x, y and z directions, as shown in Fig. 1, was 57, 79 and 34 respectively. The total number of the in-room cells was about 130000. In the horizontal direction, the grid is refined close to the source, with a cell length of 0.02 m, while after some cells it expands with a ratio of 1.08. In the vertical direction, close to the ground and to the roof, the cell height is constant at about 0.05 m and 0.1 m respectively, while it slightly expands in between. Part of the room grid and the positions of the sensors can be seen in Fig. 3. A second, coarser grid with about 65000 in-room cells was also tested.

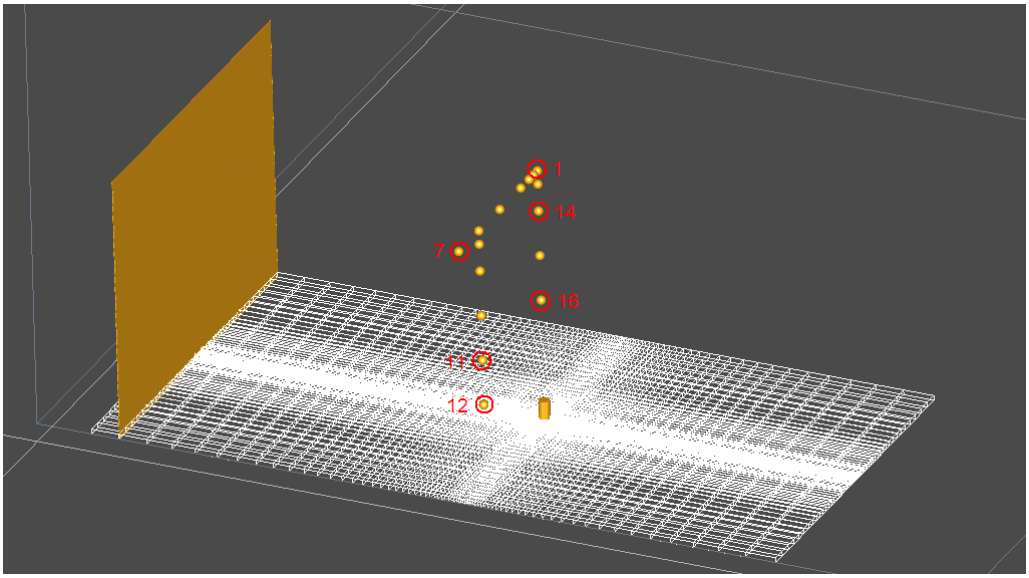

Figure 3. Ground cells of the in-room computational domain. Only the front wall is seen in the picture. Sensors for which concentration time series are provided in this document are marked.

The source is modelled as a jet surface which emits for 240 s pure hydrogen with given values of mass and momentum rates that exactly match the experimental ones. At the axis of release, zero gradient of the given values is imposed at the emitting surface. Numerically, a source term is added at the equations of the cell(s) that include the emitting surface. The walls and the ceiling, for which non-slip velocity was applied, expand for 5.9 m outside the front room wall, while at the end of the domain (at the left side, not shown in Fig. 3) Neumann boundary conditions were used. The variable time step was chosen in order to assure a maximum Courant number in the whole computational domain of CFL=0.3. This results in an average time step of dt=0.00055 s. After the end of the release, the time step increases automatically (again in order to assure CFL<0.3) and the flow partly re-laminarizes, as it can be also seen from the concentration time series.

4.0 RESULTS AND DISCUSSION

4.1 Hydrogen propagation

As it can be seen mainly from the sensors of both the experiment and the simulation, hydrogen is impetuously transferred to the top of the room, then to the lateral walls and then it accumulates at the upper part of the room, before the release stops and hydrogen stratifies and diffuses slowly.

An early snapshot of the release can be seen in Fig. 4 for both the experiment and the LES simulation.

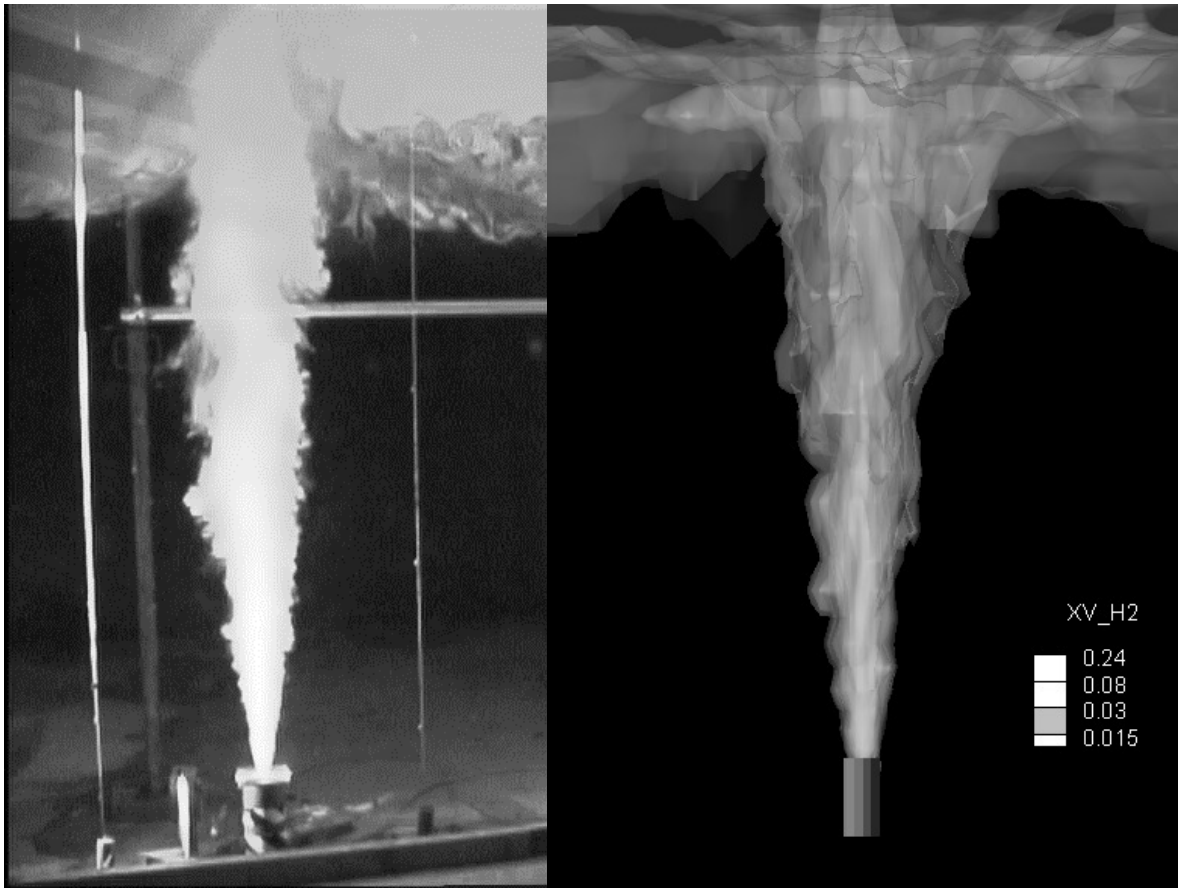

Figure 4. A photograph from an early stage of the release (left) [13] and hydrogen volume concentration isosurfaces from the LES simulation at 50 s (right).

The calculated concentration isosurfaces form patterns very similar to the experimental picture. Some details are worth to be commented though. The plume at the higher parts of the jet seems to be slightly wider in the simulation. Also, in the experiment, at this particular snapshot, the distribution of the plume at the ceiling is not symmetrical; more hydrogen is transferred towards the sensors' side of the room. That might be due to random reasons like no absolute symmetry of the geometry or of the flow and pressure conditions.

Contours of the instantaneous volume fraction concentration of the *x-z* plane that includes the jet axis, are provided in Fig. 5. The hydrogen reaches the ceiling very fast and it starts accumulating there. A flow field develops that transfers the hydrogen along the ceiling and then downwards along the side walls, which have higher concentrations than the neighboring regions of the same height. Thus the plume takes a mushroom shape. Till 240 s, constant hydrogen supply maintains a region of high concentration just above the injector, that goes up to the ceiling. After the hydrogen supply stops, this

core disappears very fast, as a result of mixing and diffusion. Throughout the procedure, the room roughly fills up with hydrogen, starting from the top to the bottom. Due to buoyancy, a more or less stratified hydrogen distribution appears after the release stops (Fig. 5, 500 s).

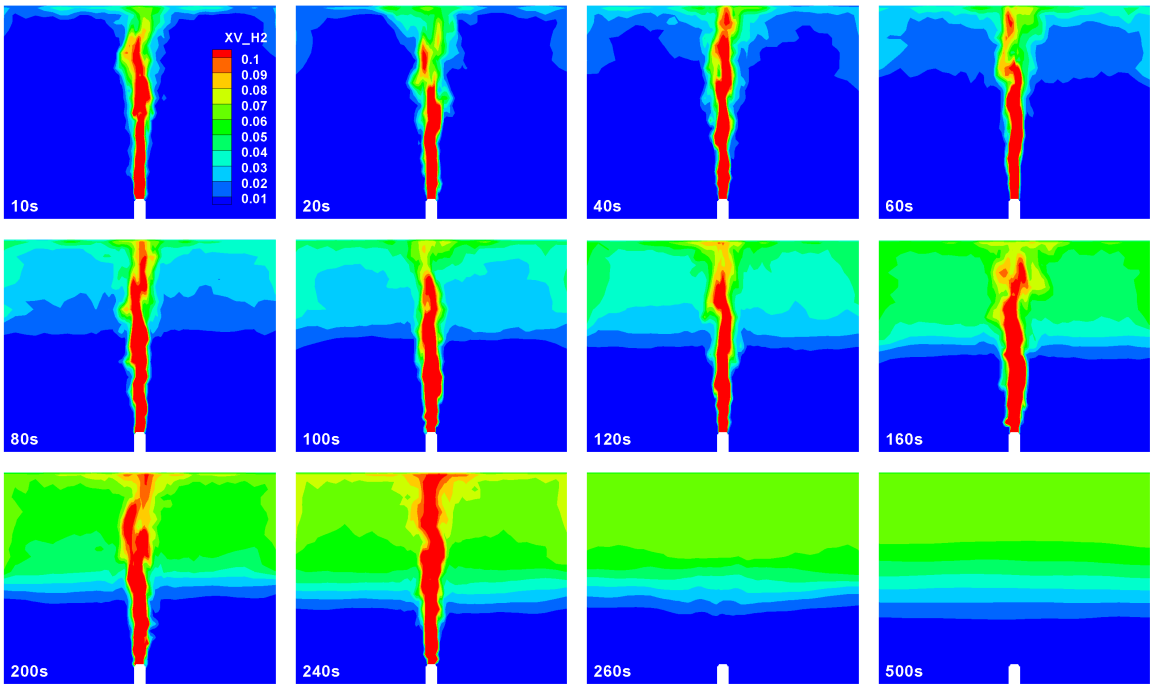

Figure 5. Hydrogen volume concentration at different times from the beginning of the release.

4.2 Comparison of measured and LES concentrations

Fig. 6 provides a comparison of measured and calculated with LES concentration time series at some sensors. Previous RANS results with ADREA-HF are also included for comparison. Details concerning the RANS simulations can be found in the SBEP-V3 intercomparison exercise [7], where ADREA-HF gave concentrations closer to the experimental ones than the average RANS results of the particular exercise. In table 1, some information concerning the grid and the computation time for both the RANS and the LES simulations is provided.

Table 1. Mesh information and computation time for LES and RANS calculations.

Methodology	Total number of cells	Minimum mesh resolution x*y	Minimum mesh resolution z	Computer run time till 500s
RANS	45356	0.02m * 0.02m	0.053m	17 hours
LES	153102	0.02m * 0.02m	0.053m	17 days
LES coarse	77894	0.02m * 0.02m	0.053m	4 days (estim.)

In Fig. 6, Sensor 16 is the first one to look, since it is the closest to the source and it gives an idea of whether the initial jets of the experiment and the simulation are the same. Sensor 14 provides information about how the vertical propagation of the plume is captured. Sensors 1 and 7 are also important, since from them the accumulation to the ceiling and the horizontal transfer of hydrogen can be seen. Sensor 12 is also very critical, since it is the lowest available and its measurements are important mainly for the second, diffusion phase of the experiment. Finally sensor 11 is above sensor 12 and at the same height with sensor 16 and adds useful information about the horizontal and vertical

differences in hydrogen concentrations. At all sensors, results from the coarser, in the x direction, LES grid are also presented in order to assess whether the grid-size effects are critical or not for the main conclusions of the present study. At the left side of Fig. 6 are the sensors which are on the jet axis.

The general comment from Fig. 6 is that the LES values compare well against the experimental data. It is noticed that current simulations were performed using the default code options and that the LES parameters, like the Smagorinsky constant C_s, were not tuned in order to better fit the measurements; Still, ADREA-HF LES predictions are better than most of the results of the SBEP-V3 intercomparison exercise [7] and also close to other fine LES calculations [14]. In [14] it is reported that with C_s=0.2 concentration values were very high and the flow had more "laminar" characteristics, due to high artificial viscosity, while a value of C_s=0.12 was successful. In consistency with that, current simulations with C_s=0.1 (close to 0.12) were successful, while a test with C_s=0.2 resulted in much higher values of concentration and significantly lower variability.

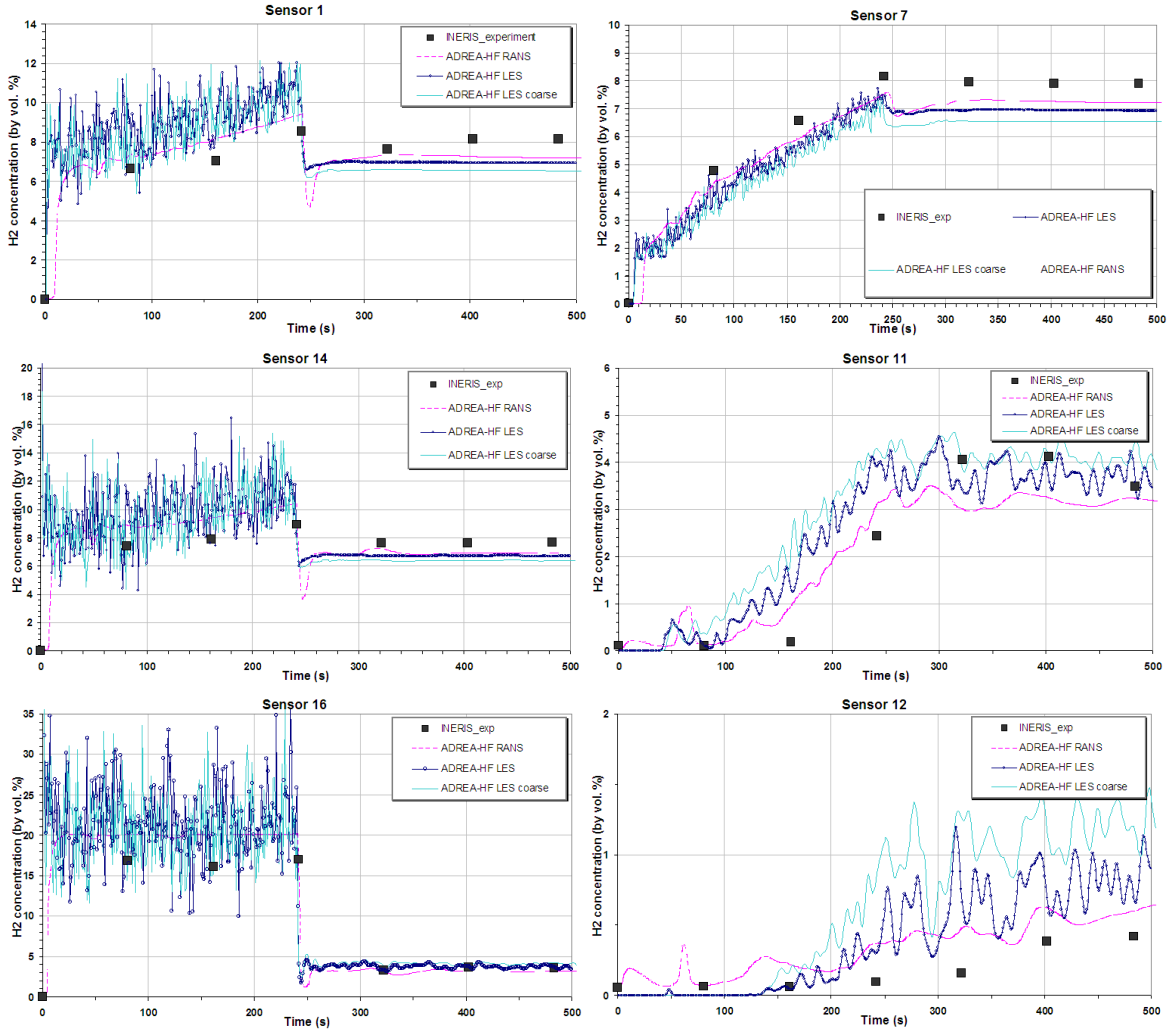

Figure 6. Experimental and computed concentration time series at various sensors

For both LES and RANS the initial hydrogen mass flow is over-estimated during the release phase, as it can be seen from sensor 16. Interestingly though, at the second (diffusion) phase of the experiment, predicted values drop down close to the measured ones and at sensor 14 even lower. That, along with similar remarks from the other sensors and from the fact that at sensor 12 the concentration is overestimated, leads to the conclusion that in CFD the diffusion is higher than it was in the

experiment. Additional evidence that favor this remark, is the wider core of hydrogen close to the ceiling that can be noticed in Fig. 4. It is believed though that, at least for the LES simulations, a finer grid or/and a more suitable Smagorinsky constant will partly correct that issue. Indeed, from most sensors it can be seen that the finer LES grid provides slightly better results. Finally, the discrepancy of underestimation (also seen at Fig. 7 of [7]) during the diffusion phase might partly be due to experimental reasons, like asymmetrical transfer of hydrogen, as it was commented earlier. More sensors, placed at the other part of the room, but also at the *y* direction might have helped in explaining this behavior.

In all sensors except sensor 12, the two phases of the experiment can be clearly distinguished. It is noticed that LES predicts very high variations of the concentration values during the first phase of the experiment at the release-axis sensors, revealing the unsteadiness of the physical phenomenon. That unsteadiness, that can partly be noticed even in Fig. 4 and Fig. 5, is not captured from RANS and of course cannot be observed at the time-averaged and sparse experimental measurements. During the release, hydrogen concentration is kept more or less constant close to the source (sensor 16), while it increases with time at bigger distances of the hydrogen transfer route (sensor 16 to 14 to 1 to 7 to 11 to 12) locations. The increase slope is in general higher the more far-away the sensor is from the source. After the supply stops, the concentration drops and that drop is higher the closer to the source. The violent turbulent flow that was triggered from the high-velocity hydrogen supply stops and the concentration variations drop considerably, especially close to the source. The hydrogen is piled to the ceiling, where it reaches a more or less constant concentration of about 8% by volume (7% from the CFD simulations).

It is noticed that RANS compares also well against the experimental values and it needs several times less computational time than LES, as it can be seen in Table 1. Of course LES has other advantages, like providing flow variations, maximum and minimum values, variances and correlations. Also, it can be more accurate in cases where RANS fails, like highly unsteady phenomena and recirculating or separated flows. Finally, in case of a potential explosion, LES has also a clear advantage over RANS, since it can offer the high variability of the instantaneous values. In general, RANS provides a more "steady-state" approach, since the equations are time-averaged, while the LES is natively unsteady and in general more suitable for transient flows.

5.0 CONCLUSIONS

The newly-added LES capability of ADREA-HF was tested for the first time in a hydrogen release application. Results are very encouraging and the code provided concentration time series close to the experimental values for all sensors. Now it is sound to say that ADREA-HF also has an LES option that can be used in hydrogen safety assessment.

The experiment used for the evaluation was the INERIS-6C, that is suggestable for CFD code validation. For such future experiments, measurements in all four directions are recommended, in order to be able to assess the symmetry in the experimental conditions.

From the results, the most important mismatch is the underestimation of CFD concentration values during the diffusion phase, even if at the release phase the hydrogen volume fraction is overestimated at the first sensor (sensor 16). There is no definite answer that fully explains this, but most probably CFD overestimates the diffusion compared to the measurements. This can be due to multiple reasons, ranged from unknown experimental parameters till the turbulence model or even the computational grid and the numerical scheme used. Some CFD options that might further improve the results, could be the fine-tuning of the Smagorinsky constant and a bigger number of more uniform cells, especially in the *z* direction.

6.0 ACKNOWLEDGEMENTS

This LES study was supported from the Greek Scholarships' Foundation and from the Municipality of Aghia Varvara Attikis, Greece.

REFERENCES

1. Bartzis, J.G., Venetsanos, A., Varvayani, M., Catsaros, N. and Megaritou, A., ADREA-I: A three-dimensional transient transport code for complex terrain and other applications, *Nuclear Technology*, **94**, 1991, pp. 135-148.
2. Venetsanos, A.G., Papanikolaou, E. and Bartzis, J.G., The ADREA-HF CFD code for consequence assessment of hydrogen applications, *International Journal of Hydrogen Energy*, **35**, 2010, pp. 3908-3918.
3. Koutsourakis, N., Venetsanos, A.G., Bartzis, J.G. and Tolias, I.C., Presentation of new LES capability of ADREA-HF CFD code, Proceedings of the 13th International Conference on Harmonisation within Atmospheric Dispersion Modelling for Regulatory Purposes, Paris, France, 1-4 June 2010, pp. 662-666.
4. Koutsourakis, N., Venetsanos, A.G., Bartzis, J.G. and Tolias, I.C., ADREA-HF code upgrade with emphasis on Large Eddy Simulation, Proceedings of the 7th panhellenic conference on fluid flow phenomena, Thessaloniki, Greece, 12-13 November 2010, pp. 163-173 (only abstract in English).
5. Koutsourakis, N., Venetsanos, A.G., Bartzis, J.G., Tolias, I.C. and Markatos, N.C., Pollutant dispersion study in asymmetric street canyons using Large Eddy Simulation, 7th GRACM International Congress on Computational Mechanics 30 June-2 July 2011, Athens, Greece (to be presented).
6. Dagba, Y., Perette, L., Venetsanos, A.G., Description of INERIS test-6 experiment and requirements for corresponding blind SBEP in the framework of the InsHyde internal project. HYSAFE report; 24 October 2005.
7. Venetsanos, A.G., Papanikolaou, E., Delichatsios, M., Garcia, J., Hansend, O.R., Heitsch, M., Huser, A., Jahn, W., Jordan, T., Lacome, J.-M., Ledin, H.S., Makarov, D., Middha, P., Studer, E., Tchouvelev, A.V., Teodorczyk, A., Verbecke, F. and Van der Voort, M.M., An inter-comparison exercise on the capabilities of CFD models to predict the short and long term distribution and mixing of hydrogen in a garage, *International Journal of Hydrogen Energy*, 2009, **34**, pp. 5912-5923.
8. Erlebacher, G., Hussaini, M.Y., Speziale, C.G. and Zang, T.A., Toward the Large-Eddy Simulation of Compressible Turbulent Flows, *Journal of Fluid Mechanics*, 1992, **238**, pp. 155-185.
9. Piomelli, U., Large-eddy and direct simulation of turbulent flows, Short course delivered at CFD2001 - 9e conférence annuelle de la Société canadienne de CFD. Kitchener, Ontario, May 2001, 70 pp. Available online from http://terpconnect.umd.edu/~ugo/research/publications.html (accessed 21-3-2011).
10. Kovalets, I.V., Andronopoulos, S., Venetsanos, A.G. and Bartzis, J.G., Optimization of the numerical algorithms of the ADREA-I mesoscale prognostic meteorological model for real-time applications, *Environmental Modelling and Software*, 2008, **23**, pp. 96-108.
11. Ferziger, J.H. and Perić, M., Computational Methods for Fluid Dynamics, 2002, 3rd Edition, Springer-Verlag, Berlin.
12. Saad, Y., Iterative methods for sparse linear systems, 2003, 2nd Edition, SIAM, Philadelphia, PA.
13. URL: http://gexconus.com/index.cfm?id=230327 (accessed 13-4-2011).
14. Zhang, J., Delichatsios, M.A. and Venetsanos, A.G., Numerical studies of dispersion and flammable volume of hydrogen in enclosures, *International Journal of Hydrogen Energy*, 2010, **35**, pp. 6431-6437.